APPLIED PHYSICS LETTERS **95**, 081904 (2009)

Highly dense amorphous Nb_2O_5 films with closed nanosized pores

M. Vinnichenko,[1,a)] A. Rogozin,[1] D. Grambole,[1] F. Munnik,[1] A. Kolitsch,[1] W. Möller,[1]
O. Stenzel,[2] S. Wilbrandt,[2] A. Chuvilin,[3] and U. Kaiser[3]
[1]*Institute of Ion Beam Physics and Materials Research, Forschungszentrum Dresden-Rossendorf, 01314 Dresden, Germany*
[2]*Fraunhofer Institut Angewandte Optik und Feinmechanik, 07745 Jena, Germany*
[3]*Universität Ulm, 89069 Ulm, Germany*

(Received 17 May 2009; accepted 5 August 2009; published online 24 August 2009)

This study is focused on tailoring the porosity of Nb_2O_5 films during reactive pulsed magnetron sputtering. Dense amorphous films containing nanopores only in deeper regions have been grown at a high rate using substrate temperatures below 60 °C. The films exhibit a high refractive index, $n_{400}=2.54$, a low extinction coefficient, $k_{400}\sim 6\times 10^{-4}$, a low mechanical stress (-90 MPa), and a negligible thermal shift. The specific depth distribution of the nanopores is believed to be the reason for the optimum trade-off between a high refractive index and low mechanical stress. © *2009 American Institute of Physics*. [DOI: 10.1063/1.3212731]

The need for cost-effective materials combining a high refractive index, low optical extinction, low mechanical stress, and amorphous homogeneous microstructure for optical applications has stimulated active research on thin films of oxides such as HfO_2, Ta_2O_5, and Nb_2O_5.[1–3] Films of Nb_2O_5 produced by magnetron sputtering remain amorphous up to a temperature of 500 °C.[4,5] In addition, their refractive index $n(\lambda=400\ \text{nm})\sim 2.60$ (Refs. 6 and 7) is significantly higher than that of HfO_2 and Ta_2O_5. However, Nb_2O_5 films with the highest refractive index, produced by either reactive pulsed magnetron sputtering (RPMS)[4] or ion plating,[8] often exhibit a relatively high compressive stress ($\sigma > 300$ MPa) (Ref. 9) and an extinction coefficient $k(\lambda=400\ \text{nm}) > 0.002$ (Refs. 6 and 7) leading to inferior performance of the resulting optical devices. There is evidence in the literature that the incorporation of nanopores may cause relaxation of the mechanical stresses in amorphous films,[4] but the pores may absorb atmospheric water, which will then lead to a thermal shift, i.e., to a thermally variable refractive index. Tailoring film porosity would enable one to achieve an optimum trade-off between mechanical and optical film properties. The volume fraction of pores in the growing film may be reduced by increasing surface adatom mobility.[10] Such an increase can be accomplished by either energetic particle bombardment or raising substrate temperature. The present study focuses on the porosity control of Nb_2O_5 films using high-growth rate RPMS with variable oxygen partial pressure, different magnetron-substrate configurations, and substrate temperatures.

Nb_2O_5 films of a thickness of 490 to 550 nm were deposited by RPMS using two 2 in. unbalanced magnetrons (MightyMAK, U.K.) operated in parallel[11] and equipped with high purity (99.95%) Nb metallic targets (Kurt J. Lesker, U.K.). The films were grown using either two magnetrons with axes directed to the sample holder edges (off-normal deposition, with the angle between the magnetron axis and the substrate normal being 17°)[11] or a single magnetron with an axis perpendicular to the substrate. The substrates were either $(10\times 10\times 0.5)$ mm^3 plates of UV-grade fused silica, $(20\times 20\times 0.3)$ mm^3 plates of crystalline Si(100), or 3 –in. wafers of crystalline Si. The substrates were at floating potential while their temperature, T_S, was kept either below 60 °C (no intentional heating) or at a fixed value of 370 °C by means of a sample holder with a boralectric heater (Tectra, Germany). In both cases, the distance from the magnetron to the substrate was 55 mm. The magnetrons were operated in a constant power mode (400–625 W per magnetron), with voltage and current values in the range of 175–500 V and 0.8–3.6 A, respectively, and frequencies of 5 and 16.67 kHz. The chamber was baked to reach a base pressure of 3.0×10^{-7} mbar before deposition. The magnetron targets were initially presputtered in pure Ar for 5 min followed by stabilization of the discharge current and gas partial pressures upon addition of O_2. Before striking the magnetron discharge, the partial pressures of Ar ($p_{Ar}=2.29\times 10^{-2}$ mbar) and O_2 [$p_{O_2}=(3.03-6.68)\times 10^{-3}$ mbar] were monitored precisely with a capacitance gauge (Pfeiffer CMR 275).

An automated Langmuir probe (SmartProbe, Scientific Systems Ltd., USA) was employed to determine the spatial distribution of the plasma ion density, N_i, with a resolution of 1 cm in the plane parallel to the substrate at a distance of 3 cm from the latter. The film optical properties were characterized using an M-2000 spectroscopic ellipsometer (J.A. Woolam Co Inc., USA) at a photon energy of 1.24–3.4 eV. Spectroscopic ellipsometry (SE) data were processed with the aid of WVASE software, and were fitted to a four-layer model involving air, surface roughness, the oxide film, and the substrate. The surface roughness was modeled using a 50% air and 50% bulk oxide Bruggeman effective medium approximation.[12] The Nb_2O_5 complex refractive index, $N=n+ik$, being consistent with the Kramers–Kronig relations, was obtained using a Cody–Lorentz parameterized model.[3] Adding a linear grading of n and k values does not improve substantially fit results for optimized Nb_2O_5 films; however, it decreases the fit mean square error by a factor of 2–3 for unoptimized ones. In the latter case, the film parameters, including thickness-averaged n values, match (within the experimental error) those obtained by a simpler model. The

[a)]Author to whom correspondence should be addressed. Electronic mail: m.vinnichenko@fzd.de. Tel.: +49 (0) 351 260 2374. FAX: +49 (0) 351 260 2703.

 © 2009 American Institute of Physics

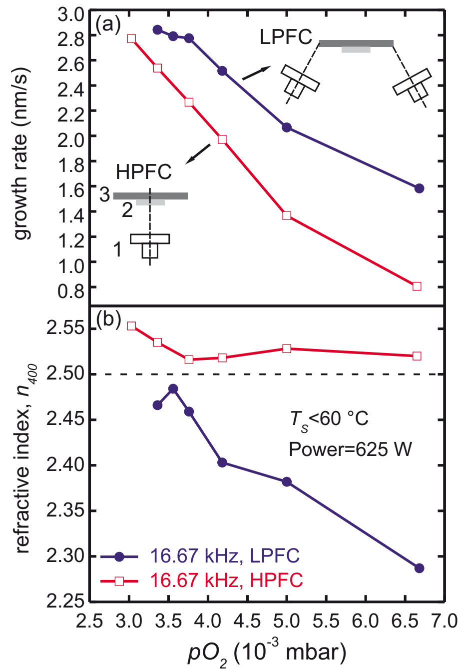

FIG. 1. (Color online) Growth rate (a) and refractive index, n_{400} (b), of films produced at different oxygen partial pressures, a substrate temperature of $T_s < 60$ °C, and magnetron power of 625 W. The insets show the configuration of the magnetron (1) with respect to the substrate (2) fixed to the substrate holder (3).

values of the refractive index and the extinction coefficient at a wavelength of 400 nm (3.1 eV), n_{400} and k_{400}, respectively, were compared for different samples, and the error involved in the former did not exceed $\Delta n_{400} \sim \pm 0.01$. The sensitivity limit of the SE measurement of the extinction coefficient was estimated to be about $k_{400} \sim 5 \times 10^{-4}$. For selected samples, the thermal shift was determined from transmission measurements with an OptiMon spectrophotometer as the relative change in the refractive index due to heating in a vacuum from room temperature to 100 °C.[13] The film stress was evaluated with Stoney's equation measuring the change in the curvature of the 3 in. Si wafers.[13] Negative and positive values correspond to tensile and compressive stress, respectively.

The hydrogen depth profile in the films was determined by nuclear reaction analysis (NRA) using $^{15}N^{2+}$ ions at energies above 6.3 MeV. The microstructure of selected films was characterized by high-resolution cross-sectional transmission electron microscopy (X-TEM) using a CM20 instrument (Philips, Netherlands) at an acceleration voltage of 200 kV, resulting in a point-to-point resolution of 0.25 nm. X-TEM specimen preparation followed a standard procedure described in more detail elsewhere.[14] The ion energy and the angle were chosen in such a way as to minimize ion milling artifacts.

Figure 1 shows the dependence of the growth rate (a) and the refractive index, n_{400}, (b) on the oxygen partial pressure p_{O_2} for films grown using two different magnetron-substrate configurations. The films were deposited on unheated substrates ($T_S < 60$ °C) at the highest magnetron power of 625 W. In the case of two magnetrons and off-normal deposition, the ion density at the substrate center is $N_i \sim 3 \times 10^{10}$ cm^{-3}. This is denoted as a low plasma flow configuration (LPFC). In the high plasma flow configuration (HPFC) for a single magnetron with an axis perpendicular to the substrate surface, the central beam of the unbalanced magnetron provides an ion density at the substrate of $N_i \geq 2.8 \times 10^{11}$ cm^{-3} for the entire range of p_{O_2} and at the two frequencies used. Increasing p_{O_2} causes a reduction in the film growth rate from 2.84 to 1.58 nm/s for LPFC, and a decrease from 2.77 to 0.80 nm/s for HPFC due to stronger coverage of the Nb magnetron target with an oxide layer resulting from an increased supply of oxygen.[15] For LPFC, the films grown at $p_{O_2} = 3.56 \times 10^{-3}$ mbar exhibit a highest refractive index of $n_{400} = 2.48$ and a relatively high extinction coefficient $k_{400} = 0.02$ (not shown). These parameters decrease to $n_{400} = 2.29$ and $k_{400} < 0.001$ at $p_{O_2} = 6.68 \times 10^{-3}$ mbar. In contrast, films grown at HPFC have a refractive index $n_{400} = 2.52 - 2.55$ and $k_{400} < 6 \times 10^{-4}$ over the whole range of p_{O_2}. In case of deposition onto heated substrates ($T_S = 370$ °C) at LPFC, a reduced magnetron power of 500 W and operation frequency of 5 kHz ($p_{O_2} = 3.36 \times 10^{-3}$ mbar) were necessary to achieve an optimum combination of a high refractive index ($n_{400} = 2.46$) and a low extinction coefficient ($k_{400} < 5 \times 10^{-4}$).

The films grown for HPFC without substrate heating (Table I) have a low tensile stress of −90 MPa and a negligible thermal shift in +0.06% in addition to high n. In contrast, the films grown for LPFC, but at an elevated substrate temperature, show a higher tensile stress (−132 MPa) and a much larger thermal shift in −2.0%.

Figure 2 shows X-TEM images of the films grown without heating for HPFC [(a)–(c)] and onto heated substrates for LPFC [(d)–(f)]. The common feature of both types of films is the dense nonporous amorphous layer near the Nb_2O_5/Si interface, with a thickness of ~5 nm [sample A, Fig. 2(c)] and ~5 nm [sample B, Fig. 2(f)]. Then, in the first case, a 10 nm thick layer consisting of isolated pores [Fig. 2(c)] forms followed by a dense amorphous microstructure with discontinuous vertical arrays of pores [Fig. 2(a)]. The characteristic pore size is 2 nm. The NRA depth profile shows that the hydrogen content in the film decreases from 1.2 at. % at the surface to values below the detection limit inside the film. The low hydrogen content is mainly attributed to atmospheric water adsorption at the surface rather than to water uptake by the pores. Accordingly, the thermal shift becomes negligible.

Conversely, for LPFC on heated substrates, no such a porous layer is observed near the film-substrate interface, and vertical arrays of pores start to form directly from the

TABLE I. Deposition parameters, thermal shift, and stress of the two different series of Nb_2O_5 samples.

Sample	T_S (°C)	P_m (W)	V_m (V)	f_m (kHz)	No. of magnetrons	N_i (10^{11} cm^{-3})	Configuration	Thermal shift (%)	Stress (MPa)
A	<60	625	175	16.67	1	2.8	HPFC	+0.06	−90
B	370	500	500	5	2	0.08	LPFC	−2.0	−132

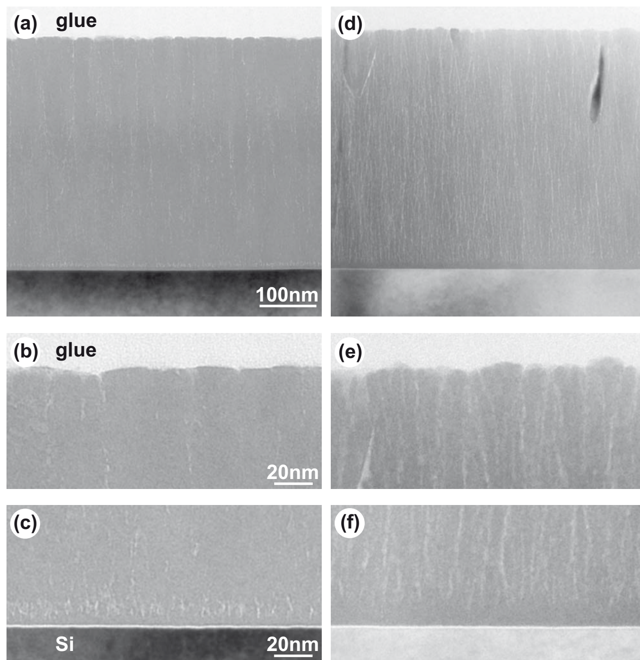

FIG. 2. X-TEM images of films grown onto unheated substrates in HPFC mode [(a)–(c)], and at T_S=370 °C in LPFC mode [(d)–(f)].

dense area [Figs. 2(d) and 2(f)], then continue through the film and, finally, open at the film surface [Fig. 2(e)]. The characteristic pore size is a little larger than described above, i.e., ~3 nm, while the pore density is significantly higher. These findings are in agreement with the NRA depth profile showing a high H concentration decreasing from 11 to 7 at. % with film thickness. The significant uptake of atmospheric water by the open pores explains the high thermal shift observed in these films.

The increased particle bombardment for HPFC at normal incidence is the reason for the observed formation of a dense amorphous microstructure with a small volume fraction of closed nanosized pores. In our case of reactive unbalanced magnetron sputtering, positive plasma ions contribute appreciably to the thermal power at the substrate[16] for plasma ion densities higher than 10^{11} cm^{-3}. In addition, energetic reflected neutral particles of Ar might play a role because their mass is appreciably lower than that of Nb target atoms. Since the refractive index of the material correlates with its density,[5] the densification of the amorphous film produces the high n values obtained irrespectively of p_{O_2}, and occurs for $N_i > 10^{11}$ cm^{-3}. The decreased particle bombardment for LPFC, as indicated by the low plasma ion density ($N_i \sim 10^{10}$ cm^{-3}), in conjunction with off-normal deposition, favors shadowing effects which in turn lead to the porous microstructure observed even in the case of growth at an elevated substrate temperature T_S=370 °C. A higher degree of porosity explains the lower refractive index values of the films grown for LPFC in comparison with those for HPFC (Fig. 1).

The influence of the nanosized pores on the film refractive index, thermal shift, and mechanical stress in the amorphous Nb_2O_5 films is interpreted in light of a recently developed model.[17] It is assumed that nonporous films show a high refractive index and a zero thermal shift while having a high compressive stress. The model suggests that there is an optimum volume fraction of closed pores of about 1% and, while the refractive index is still high, the film has a low stress and a thermal shift close to zero. The properties of the Nb_2O_5 samples deposited for HPFC match closely the predictions of this model, thus providing an optimum trade-off between the discussed optical and mechanical film parameters. Further enhancement in porosity and dominance of open pores increase the tensile stress, reduce significantly the refractive index, and lead to a substantial negative thermal shift. This situation corresponds to the films produced at LPFC.

n_{400}=2.54 (n_{550}=2.36) is among the highest refractive index values achieved to date using magnetron sputtering[4] and is only a little below the value n_{550}=2.40 for films produced by ion plating.[8] However, the films with the highest refractive index in Ref. 4 exhibit a mechanical stress of −200 MPa while ion plated films show an extinction coefficient in the visible spectral range of $k_{515}=5\times10^{-4}$ (Ref. 8) which is commensurate with our values in the UV spectral range. In addition, the growth rate of the films studied in the present work is the highest compared to the values available in literature.[4,8]

In summary, adjusting the deposition geometry and plasma ion density during RPMS enables one to tailor the porosity of amorphous Nb_2O_5 thin films using a three-dimensional growth mode. Films with a low extinction coefficient, a high refractive index, low tensile stress and negligible thermal shift have been obtained during deposition for plasma ion densities above 10^{11} cm^{-3} and substrate temperatures below 60 °C. These properties have been explained by the formation of a dense amorphous microstructure with a specific depth distribution of closed nanopores. In contrast, films grown at 370 °C using low plasma ion densities (~10^{10} cm^{-3}) are less dense with pores being open at the film surface, and show a significant thermal shift, higher tensile stress and lower refractive index.

The authors gratefully acknowledge assistance of R. Yankov and financial support by the EFDS and AiF Project No. 15042 BR “NANOMORPH.”

[1]L. Martinu and D. Poitras, J. Vac. Sci. Technol. A **18**, 2619 (2000).
[2]J. M. Ngaruiya, O. Kappertz, S. H. Mohamed, and M. Wuttig, Appl. Phys. Lett. **85**, 748 (2004).
[3]J. Price, P. Y. Hung, T. Rhoad, B. Foran, and A. C. Diebold, Appl. Phys. Lett. **85**, 1701 (2004).
[4]B. Hunsche, M. Vergöhl, H. Neuhäuser, F. Klose, B. Szyszka, and T. Matthee, Thin Solid Films **392**, 184 (2001).
[5]S. Venkataraj, R. Drese, Ch. Liesch, O. Kappertz, R. Jayavel, and M. Wuttig, J. Appl. Phys. **91**, 4863 (2002).
[6]M. G. Krishna and A. K. Bhattacharya, Int. J. Mod. Phys. B **13**, 411 (1999).
[7]M. Vergöhl, B. Hunsche, N. Malkomes, T. Matthee, and B. Szyszka, J. Vac. Sci. Technol. A **18**, 1709 (2000).
[8]A. Hallbauer, D. Huber, G. N. Strauss, S. Schlichtherle, A. Kunz, and H. K. Pulker, Thin Solid Films **516**, 4587 (2008).
[9]C.-C. Lee, C.-L. Tien, and J.-C. Hsu, Appl. Opt. **41**, 2043 (2002).
[10]R. W. Smith and D. J. Srolovitz, J. Appl. Phys. **79**, 1448 (1996).
[11]A. I. Rogozin, M. V. Vinnichenko, A. Kolitsch, and W. Möller, J. Vac. Sci. Technol. A **22**, 349 (2004).
[12]D. E. Aspnes, J. B. Theeten, and F. Hottier, Phys. Rev. B **20**, 3292 (1979).
[13]O. Stenzel, S. Wilbrandt, N. Kaiser, M. Vinnichenko, F. Munnik, A. Kolitsch, A. Chuvilin, U. Kaiser, J. Ebert, S. Jakobs, A. Kaless, S. Wüthrich, O. Treichel, B. Wunderlich, M. Bitzer, and M. Grössl, Thin Solid Films **517**, 6058 (2009).
[14]J. C. Bravman and R. Sinclair, J. Electron Microsc. Tech. **1**, 53 (1984).
[15]S. Berg and T. Nyberg, Thin Solid Films **476**, 215 (2005).
[16]A. Rogozin, M. Vinnichenko, N. Shevchenko, A. Kolitsch, and W. Moeller, Thin Solid Films **496**, 197 (2006).
[17]O. Stenzel, J. Phys. D **42**, 055312 (2009).